Electronic Supporting Information†

High-purity cell-sorting centrifugal microfluidic chip with flow rectifier

Junyu Ma,[ab] Yihui Wu,*[a] Yongshun Liu,*[a] Yuan Ji,[ab] Mei Yang[c] and Hongquan Zhu[c]

In this supplementary document, we present information about the theoretical analysis of fluid motion and forces on particles, description of non-steady flow process, numerical simulation of the particle trajectory, description of the vortex in the separation chamber and the impact of deformable particles.

[a] *State Key Laboratory of Applied Optics, Changchun Institute of Optics, Fine Mechanics and Physics (CIOMP), Chinese Academy of Sciences, Changchun, China. Fax: 0431-85690271; Tel: 0431-86176135; E-mail: yihuiwu@ciomp.ac.cn; liuyongshun1981@163.com*
[b] *School of optoelectronics, University of Chinese Academy of Sciences, Beijing, China.*
[c] *Department of Clinical Laboratory, The Second Hoapital of Jilin University, Changchun, China.*

S1 Theoretical analysis of fluid motion and force on particles

In this study, the fluid in the channel tends to be steady flow state, and the average velocity of the fluid is given by[1]

$$U = \frac{Q}{S} \tag{S1}$$

where S is the cross-sectional area, and Q is the total volumetric flow rate through the channel system. In a microchannel with featuring laminar, viscous and incompressible flow, the flow rate Q is calculated by[2]

$$Q = \frac{\Delta P}{R} \tag{S2}$$

where ΔP represents a pressure gradient, and R is the hydrodynamic resistance of the entire microchannel. This resistance is determined by the cross-section of the channel, which is expressed by[3]

$$R = \frac{12\mu L}{w^3 h}[1 - \frac{w}{h}(\frac{192}{\pi^5}\sum_{n=1,3,5}^{\infty}\frac{1}{n^5}tanh(\frac{n\pi h}{2w}))]^{-1} \tag{S3}$$

L denotes the length of the channel. w and h are the channel width and height of the cross-section, respectively. In centrifugal platform, centrifugal force is of importance as driving force.[4] For convenience, the vector force mentioned before is replaced with scalar pressure difference. Thus, the pressure difference (ΔP) between two ends of radial channel filled with fluid is given by[5]

$$\Delta P = \frac{1}{2}\rho\omega^2(r_2^2 - r_1^2) \tag{S4}$$

where ρ denotes the fluid density, ω is the rotational velocity, r_1 and r_2 are the inner radial point and the outer radial point of the liquid column (see Fig.1). As mentioned before, the particles are subjected to centrifugal and Coriolis forces since the platform rotates at a constant angular speed, as shown in Fig. 1. Considering the movement of a particle at a velocity $\vec{v}_f$ from the rotation center $\vec{r}$ and the buoyancy effect on the particle under the pressure difference in the centrifugal field, the two forces can be determined as[6]

$$\vec{F}_{Cenp} = -\frac{\pi}{6} d_p^3 (\rho_p - \rho) \vec{\omega} \times (\vec{\omega} \times \vec{r}) \tag{S5}$$

$$\vec{F}_{Corp} = -\frac{\pi}{3} d_p^3 (\rho_p - \rho) \vec{\omega} \times \vec{v}_p \tag{S6}$$

where d_p is the particle diameter, $\vec{v}_p$ refers to the particle velocity vector and ρ_p is the particle density, $\vec{\omega}$ represents the rotational velocity vector. In a continuous Newtonian flow, a particle is subject to an unbalanced lateral force, which is constituted of shear gradient and wall induced lift force when the particle moves in a medium Reynolds number region in a straight channel (see Fig.1). This lateral force is expressed as[7]

$$\begin{aligned} \vec{F}_L &= \rho \frac{r_p^4}{D^2} \beta (\beta G_1(s) + \gamma G_2(s)) \vec{n} \\ \beta &= |D(\vec{n} \cdot \nabla) \vec{u}_p| \\ \gamma &= |\frac{D^2}{2} (\vec{n} \cdot \nabla)^2 \vec{u}_p| \\ \vec{u}_p &= (\vec{E} - (\vec{n} \otimes \vec{n})) \vec{u} \end{aligned} \tag{S7}$$

where r_p is the particle radius, D denotes the distance between the channel walls, $\vec{n}$ is the wall normal at the nearest point on the reference wall, s represents the normalized distance from the particle to the reference wall, divided by D so that $0 < s < 1$ for particles in the channel, G_1 and G_2 are dimensionless functions of the normalized wall distance.[7] Due to the relative motion between particles and fluid in the centrifugal field, particles will be subject to the resistant force of fluid (see Fig. 1), which can be calculated by[8]

$$F_d = 3\pi \mu d_p (\vec{u} - \vec{v}_p) \tag{S8}$$

where $\vec{u}$ is the velocity vector of the fluid.

S2 Describe of non-steady flow process

The experimental results: The liquid levels of the sample chamber at 0, 1, and 2 s are shown in Fig. S1a, b and c, respectively, which drops with time. The average velocity of the fluid can be deduced from equations (S1), (S2) and (S4) as

$$U = \frac{\rho \omega^2 (r_2^2 - r_1^2)}{2SR} \tag{S9}$$

it can be seen that the average fluid velocity decreases with the increase of the centrifugal radius r_1, which is the liquid level position. Therefore, the fluid velocity changes over time, that is, this

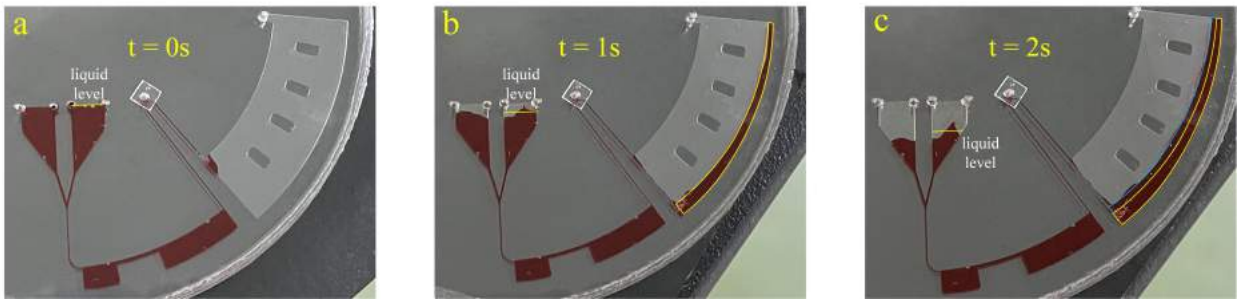

Fig. S 1 a, b, and c are the positions of the liquid level in the sample chamber without flow rectifier at 2500 rpm for 0, 1, and 2 s, respectively. The yellow frame and the blue frame in c are the increased liquid volume within 0-1 and 1-2 s, respectively.

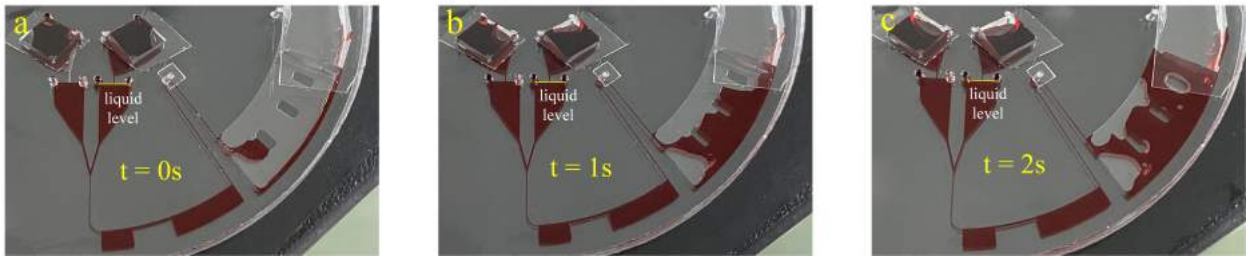

Fig. S 2 a, b, and c are the positions of the liquid level in the sample chamber with flow rectifier at 2500 rpm for 0, 1, and 2 s, respectively.

process is a non-steady flow process. In addition, it can be seen from the volume ratio of the liquid in the waste chamber in Fig. S1b and c that within the same 1 s, the flow rates are unequal and the flow rate of 1-2 s is less than that of 0-1 s, so the flow rate decreases over time.

However, for the chip with flow rectifier, the liquid levels in the sample chamber are shown in Fig. S2a, b and c at 0, 1 and 2 s, respectively. Since the flow rectifier supplements the liquid in the sample chamber, the liquid level in the sample chamber does not change over time, so the flow rate tends to be constant. Besides, it can be seen from the volume of liquid in the waste chamber with or without flow rectifier that the flow rate of the chip with flow rectifier is larger than that without flow rectifier in the same time interval (0-1 s, 1-2 s), which also shows that the flow rate of the chip with flow rectifier does not decrease over time.

S3 Numerical simulation of particle trajectory

According to the previous theoretical analysis, centrifugal force and Coriolis force are applied to the fluid in the centrifugal field, and the inlet velocity is U. Besides, Centrifugal force, Coriolis force, inertial lift force and drag force are applied to the particles. The presence of pinched flow makes particles flow in from the right of the channel. As Fig. S3a shows, large particles sedimentate in the separation chamber and small particles flow out, which is consistent with the theoretical analysis. The particle coordinates of the position of A, B and C in Fig. S3a were emphasized in Fig. S3b to characterize the trajectory of the particles precisely. Because the inertial lift force exist, from the straight channel A to B, particles are gradually move away from the right-

side wall of the channel and focus towards the middle. Therefore, particles have different certain of lateral movements, and particles of the larger sizes have more obvious movements. As the particles reach the inlet position C of the separation chamber, particles drop due to the different migration distances of the particles with different sizes under the centrifugal force and then are separated.

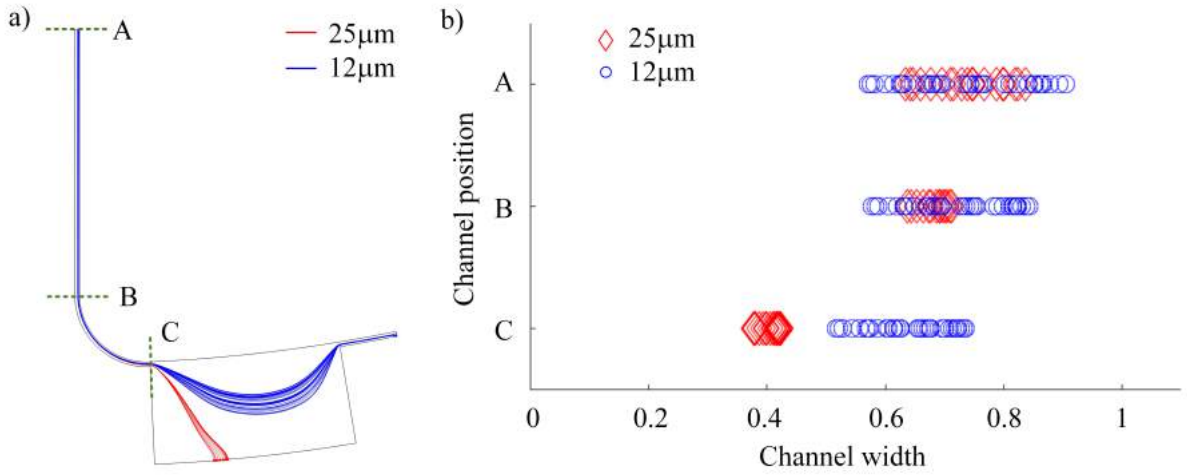

Fig. S 3 a) Numerical simulation of the particle trajectory in the pinched flow channel and the separation chamber. The red is 25 μm particles sedimentating in the separation chamber, and the blue is 12 μm particles flowing out of the separation chamber. b) Particles distribution at positions A, B, and C of the pinched flow channel.

S4 Vortex in the separation chamber

The Reynolds number is defined as $R_e = \rho U_{max} H/\mu$, where U_{max} is the maximum fluid velocity, H is the channel dimension prior to the expansion hydraulic diameter which can be calculated as $2wh/(w+h)$ in a rectangular channel. In Fig. S4, variations in vortex formation are illustrated with differing Reynolds numbers. The channel Reynolds numbers of 10, 14, and 18 are calculated using the channel dimension prior to the expansion, and they correspond to rotation speeds of 3000, 3500, and 4000 rpm, respectively.

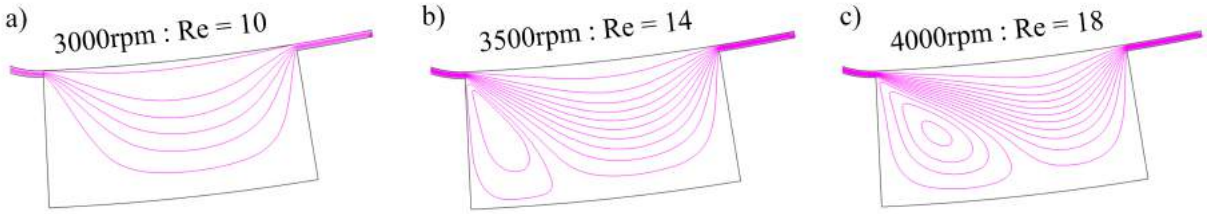

Fig. S 4 Numerical simulation of vortex in the separation chamber. a), b), and c) are the Reynolds number and the size of the vortex in the separation chamber at 3000, 3500, and 4000 rpm, respectively.

S5 The impact of deformable particles

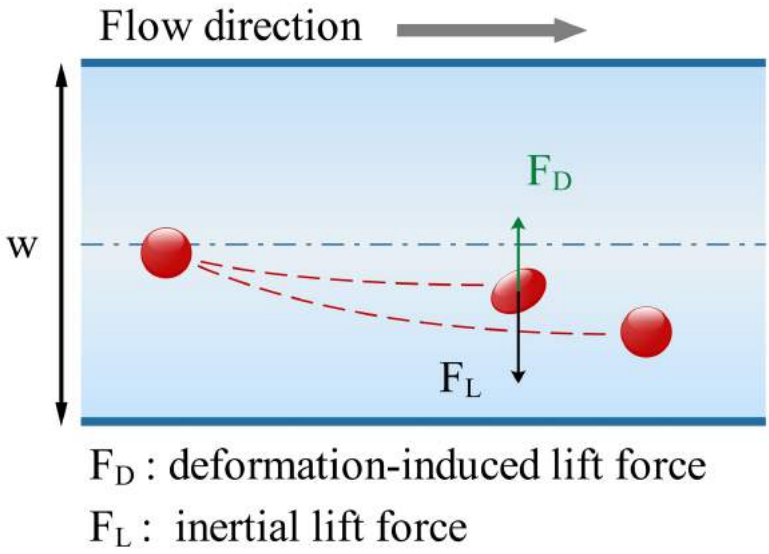

Fig. S 5 Two lateral forces on deformable particles in microchannel, namely inertial lift force, F_L, and deformation-induced force, F_D.

Notes and references

[1] T. Morijiri, M. Yamada, T. Hikida and M. Seki, *Microfluidics and Nanofluidics*, 2013, **14**, 1049–1057.

[2] R. Martinez-Duarte, R. A. Gorkin III, K. Abi-Samra and M. J. Madou, *Lab Chip*, 2010, **10**, 1030–1043.

[3] M. Yamada, J. Kobayashi, M. Yamato, M. Seki and T. Okano, *Lab Chip*, 2008, **8**, 772–778.

[4] T. Minghui, W. Guanghui, K. Siu-Kai and H. Ho-Pui, *Micromachines*, 2016, **7**, 26.

[5] O. Strohmeier, M. Keller, F. Schwemmer, S. Zehnle, D. Mark, F. von Stetten, R. Zengerle and N. Paust, *Chem. Soc. Rev.*, 2015, **44**, 6187–6229.

[6] M. Madadelahi, L. F. Acosta-Soto, S. Hosseini, S. O. Martinez-Chapa and M. J. Madou, *Lab Chip*, 2020, **20**, 1318–1357.

[7] B. P. Ho and L. G. Leal, *Journal of Fluid Mechanics*, 1974, **65**, 365–400.

[8] Y. Zhou, Z. Ma and Y. Ai, *RSC Adv.*, 2019, **9**, 31186–31195.